AJNR

Normalized Parameters of Dynamic Contrast-Enhanced Perfusion MRI and DWI-ADC for Differentiation between Posttreatment Changes and Recurrence in Head and Neck Cancer

A. Baba, R. Kurokawa, E. Rawie, M. Kurokawa, Y. Ota and A. Srinivasan

Normalized Parameters of Dynamic Contrast-Enhanced Perfusion MRI and DWI-ADC for Differentiation between Posttreatment Changes and Recurrence in Head and Neck Cancer

A. Baba, R. Kurokawa, E. Rawie, M. Kurokawa, Y. Ota, and A. Srinivasan

ABSTRACT

BACKGROUND AND PURPOSE: Differentiating recurrence from benign posttreatment changes has clinical importance in the imaging follow-up of head and neck cancer. This study aimed to investigate the utility of normalized dynamic contrast-enhanced MR imaging and ADC for their differentiation.

MATERIALS AND METHODS: This study included 51 patients with a history of head and neck cancer who underwent follow-up dynamic contrast-enhanced MR imaging with DWI-ADC, of whom 25 had recurrences and 26 had benign posttreatment changes. Quantitative and semiquantitative dynamic contrast-enhanced MR imaging parameters and ADC of the ROI and reference region were analyzed. Normalized dynamic contrast-enhanced MR imaging parameters and normalized DWI-ADC parameters were calculated by dividing the ROI by the reference region.

RESULTS: Normalized plasma volume, volume transfer constant between extravascular extracellular space and blood plasma per minute (K^{trans}), area under the curve, and wash-in were significantly higher in patients with recurrence than in those with benign posttreatment change ($P = .003$ to $<.001$). The normalized mean ADC was significantly lower in patients with recurrence than in those with benign posttreatment change ($P < .001$). The area under the receiver operating characteristic curve of the combination of normalized dynamic contrast-enhanced MR imaging parameters with significance (normalized plasma volume, normalized extravascular extracellular space volume per unit tissue volume, normalized K^{trans}, normalized area under the curve, and normalized wash-in) and normalized mean ADC was 0.97 (95% CI, 0.93–1).

CONCLUSIONS: Normalized dynamic contrast-enhanced MR imaging parameters, normalized mean ADC, and their combination were effective in differentiating recurrence and benign posttreatment changes in head and neck cancer.

ABBREVIATIONS: AUC = area under the curve; AUROCC = area under the receiver operating characteristic curve; DCE = dynamic contrast-enhanced; EES = extravascular extracellular space; Kep = rate transfer constant between EES and blood plasma per minute; K^{trans} = volume transfer constant between extravascular extracellular space and blood plasma per minute; n- = normalized; Ve = extravascular extracellular space volume per unit tissue volume; Vp = plasma volume; WI = wash-in; WO = washout

The main aims of imaging evaluation in the follow-up of head and neck cancer after treatment are to determine the effect of treatment, evaluate disease control, and detect local recurrence. Local recurrence is one of the most clinically important forms of recurrence in head and neck cancer,[1] and its early detection is important because it leads to subsequent salvage therapy. Posttreatment changes such as edema, inflammation, and fibrosis may cause difficulty in differentiating recurrences from benign posttreatment changes during follow-up imaging evaluation,[2-4] and tissue biopsy may be required for pathologic confirmation in some patients. Contrast-enhanced CT and PET/CT are the principal imaging modalities for posttreatment evaluation of head and neck cancer;[5] however, patients may undergo MR imaging when it is difficult to distinguish between recurrence and posttreatment changes.

Dynamic contrast-enhanced MR imaging (DCE-MR imaging) is a perfusion imaging technique that uses contrast media and has many important utilities in the pre- and posttreatment evaluation of head and neck cancer.[6-15] Although several studies using DCE-MR imaging have reported the utility of semiquantitative[13,14,16,17] or quantitative parameters such as permeability surface area and

blood volume[12] for differentiating head and neck cancer recurrence from benign posttreatment changes, there have been no studies that used the relatively new vascular permeability parameters, such as fractional plasma volume (Vp), extravascular extracellular space (EES) volume per unit tissue volume (Ve), volume transfer constant between EES and blood plasma per minute (K^{trans}), and rate transfer constant between EES and blood plasma per minute (Kep), or normalized DCE-MR imaging parameters that consider intervendor and interinstitutional reproducibility.

DWI is a unique sequence of noninvasive MR imaging used to visualize changes in the molecular motion of water and is a surrogate marker for cell density. DWI parameters, especially ADC, were lower in the recurrence of head and neck cancers than in benign changes after treatment.[18-20] To date, there have been no studies that have investigated the differentiation between head and neck cancer recurrences and posttreatment changes using normalized DWI-ADC that also consider intervendor and interinstitutional reproducibility as in the previously described normalized DCE-MR imaging parameters.

This study aimed to evaluate the difference in normalized quantitative and semiquantitative parameters and the normalized DWI-ADC between recurrences and benign posttreatment changes in head and neck cancer and to investigate the combined diagnostic performance of normalized DCE-MR imaging parameters and normalized DWI-ADC.

MATERIALS AND METHODS

We obtained the institutional review board exemption of University of Michigan for this retrospective study, and patient consent was waived. Data were acquired in compliance with all applicable Health Insurance Portability and Accountability Act regulations. All procedures followed were in accordance with Helsinki Declaration of 1975, as revised in 2008. Data were de-identified before any analysis.

Patients

Consecutive patients with a history of head and neck cancers from January 2014 to September 2020 who underwent follow-up DCE-MR imaging were searched by the electronic database of our institution. Seventy-seven patients whose primary malignancies were previously treated were included in this study. In our institution, all postoperative MR imaging protocols for patients with a history of head and neck malignancy include DCE-MR imaging except for patients with limitations such as intolerance to the test, contrast allergy, and narrow veins preventing bolus injection. One patient in whom postoperative changes could not be identified on MR imaging was excluded. Seven patients in whom DWI-ADC was difficult to evaluate due to artifacts and 3 patients in whom DWI-ADC of the neck region was not performed were excluded. Fifteen patients for whom an MR imaging vendor was used other than the one included in this study were excluded. Fifty-one patients matched the selection criteria (Online Supplemental Data). All patients were classified into 2 groups: the recurrence group and the benign posttreatment change group. Patients were included in the recurrence group if they had pathologic or unequivocal radiologic evidence, including follow-up examination or [^{18}F] FDG-PET/CT, of recurrent malignancy. Patients were included in the benign posttreatment change group if they had no pathologic evidence of recurrent malignancy or showed stable or improved imaging findings for >1 year.

MR Imaging Acquisition

MR imaging examinations were performed using 1.5T ($n = 33$) and 3T ($n = 18$) MR imaging systems (Ingenia, Achieva; Philips Healthcare). DWI was performed with b-values of 0 and 1000 s/mm^2 and the following parameters: TR range, 10,000–4000 ms; TE range, 98–55 ms; number of excitations, 1–2; section thickness/gap, 3.5–6/–1–1 mm; FOV, 225–255 × 225–255 mm; matrix, 120–200 × 120–200; and 3 diffusion directions. DCE-MR imaging scans were obtained via 3D T1-weighted fast-field echo. Parameters for 3D T1-weighted fast-field echo were as follows: TR, 4.8 ms; TE, 2 ms; flip angle, 30°; section thickness/gap, 5/–2.5 mm; FOV, 240 × 240 mm; matrix, 240 × 240; number of excitations, 1; number of slices per dynamic scan, 48; temporal resolution, 8.8 seconds; total acquisition time, 4 minutes 24 seconds. An intravenous bolus of 20 mL of gadobenate dimeglumine contrast (MultiHance; Bracco Diagnostics) was administered through a peripheral arm vein using a power injector with a flow rate of 5.0 mL/s, followed by a 20-mL saline flush.

Patients Demographics

The patient demographics, including age, sex, subsite, and histologic diagnosis of primary cancer, treatment method, and the reference method of recurrences or posttreatment changes, were reviewed from the electronic medical records.

ADC Analysis

ADC maps were constructed by a monoexponential fitting model using available software (Olea Sphere, Version 3.0; Olea Medical). Two head and neck radiologists with 11 and 20 years of experience outlined 3 separate ROIs on the ADC maps, predominantly including the low-signal-intensity region while excluding cystic or necrotic regions from ROIs with consensus. Another ROI was placed as a reference in the spinal cord, which was included in the FOV of every study.[21] For each ROI, normalized (n-) mean ADC (nADC$_{mean}$) was calculated by dividing the mean ADC by the reference mean ADC of the spinal cord. The values of mean ADC and nADC$_{mean}$ of 3 ROIs were averaged.

Quantitative and Semiquantitative DCE Analysis

Quantitative DCE-MR imaging analyses were performed using Olea Sphere, Version 3.0, based on the extended Tofts model, by which pixel-based parameter maps are calculated from time-intensity curves. An arterial input function was calculated automatically using cluster analysis techniques, and deconvolution of the arterial input function was performed with a time-insensitive block-circulant singular-value decomposition.[22] The 2 head and neck radiologists outlined 3 separate ROIs in the lesions on permeability maps, predominantly including the enhancing components while excluding cystic or necrotic regions from the ROIs with consensus. The calculated quantitative parameters were Vp, Ve, K^{trans}, and Kep. Semiquantitative analysis was also performed using the same ROIs described above using the Olea Sphere 3.0 software. The average signal intensity within the ROIs was plotted

DCE-MR imaging and ADC parameters

	Recurrence (n = 25) (Median [Range])	Benign Posttreatment Change (n = 26) (Median [Range])	P Value
DCE parameters			
Vp	0.09 (0.02–0.22)	0.05 (0.01–0.14)	
Reference Vp	0.01 (0.01–0.04)	0.02 (0.01–0.05)	
nVp	7.00 (0.50–17.33)	2.02 (0.33–14.33)	.003[a]
Ve	0.39 (0.07–0.98)	0.28 (0.01–1.08)	
Reference Ve	0.14 (0.01–0.26)	0.19 (0.07–0.67)	
nVe	2.55 (0.32–97.66)	1.56 (0.01–6.35)	.014
K^{trans}	0.25 (0.06–1.02)	0.13 (0.01–0.39)	
Reference K^{trans}	0.08 (0.01–0.15)	0.11 (0.04–0.33)	
nK^{trans}	3.87 (0.66–101.00)	1.27 (0.03–8.00)	<.001[a]
Kep	0.61 (0.39–2.03)	0.50 (0.16–2.12)	
Reference Kep	0.48 (0.02–1.36)	0.55 (0.32–1.06)	
nKep	1.45 (0.47–26.17)	0.96 (0.28–2.69)	.009
AUC	28,265 (3523–427,571)	11,887 (537–335,025)	
Reference AUC	7119 (615–188,345)	7890 (3530–185,938)	
nAUC	3.34 (1.31–20.81)	1.39 (0.01–9.96)	<.001[a]
WI	1.03 (0.29–2102.33)	0.70 (0.06–38.00)	
Reference WI	0.38 (0.02–696.00)	0.33 (0.07–21.24)	
nWI	4.13 (0.99–20.17)	1.70 (0.07–32.48)	<.001[a]
WO	0.68 (0.01–472.33)	0.57 (0.01–18.99)	
Reference WO	0.08 (0.01–117.00)	0.43 (0.02–27.28)	
nWO	3.78 (0.31–292.88)	1.35 (0–109.00)	.016
ADC value	1.01 (0.55–1.30)	1.61 (1.02–2.53)	
Reference ADC	0.79 (0.56–0.94)	0.78 (0.67–0.99)	
$nADC_{mean}$	1.31 (0.77–1.65)	2.07 (1.39–3.04)	<.001[a]

[a] Statistically significant.

against time, and time-intensity curves were constructed. The following parameters were calculated on a pixel-by-pixel basis from the time-intensity curves: area under the curve (AUC; the relative quantity of contrast agent across time), wash-in (WI; velocity of enhancement), and washout (WO; velocity of enhancement loss). For each ROI, normalized DCE-MR imaging parameters were calculated by dividing the mean value within the ROI placed in the lesion by the mean value within the reference ROI placed in the muscle tissue. The values of normalized DCE-MR imaging quantitative and semiquantitative parameters of the 3 ROIs were averaged.

Statistics

Shapiro-Wilk tests were performed to confirm the normality of distribution in each parameter. The Mann-Whitney U test was used to compare normalized DCE-MR imaging quantitative and semiquantitative parameters (nVp, nVe, nK^{trans}, nKep, nAUC, nWI, and nWO), age, and $nADC_{mean}$ between the recurrences and benign treatment changes. Sex was compared between the recurrences and benign treatment changes using the Fisher exact test. For parameters that showed a statistically significant difference, the optimal cutoff values in receiver operating characteristic analysis were determined as a value to maximize the Youden index (sensitivity + specificity −1). Diagnostic performances were calculated on the basis of the cutoff values. Several parameters that were significantly different in the univariate analysis described above were combined by logistic regression analysis to calculate the area under the receiver operating characteristic curve (AUROCC) as a combined parameter. Family-wise error–corrected 2-sided P values < .05 were considered statistically

significant. Family-wise error correction was performed by the Bonferroni method. All statistical analyses were performed using R, Version 3.6.1 (http://www.r-project.org/).

RESULTS

Fifty-one patients were included in the study, of whom 25 had recurrence and 26 had benign posttreatment changes. The results of demographic and clinical data are summarized in the Online Supplemental Data. The most common sites of primary cancer were major salivary glands (14/51, 27.5%), sinonasal cavity (11/51, 21.6%), oral cavity (10/51, 19.6%), nasopharynx (8/51, 15.7%), and oropharynx (6/51, 11.8%). The histology of primary cancer mainly consisted of squamous cell carcinoma (26/51, 51%), adenoid cystic carcinoma (13/51, 25.5%), and mucoepidermoid carcinoma (7/51, 13.7%). The most common treatment methods were surgery and radiation therapy (15/51, 29.4%), followed by chemoradiotherapy (14/51, 27.5%) and surgery (14/51, 27.5%). The reference method of recurrence was mostly performed by pathology correlation (20/26, 76.9%), and the reference method of benign posttreatment changes was mainly by imaging follow-up (21/25, 84%). No significant differences in median patient age were found between the recurrence and benign posttreatment change groups (65 years; range, 21–89 years) versus 57.5 years (range, 22–77 years), respectively ($P = .25$). No significant differences in sex were found between the recurrence and benign posttreatment groups (male/female, 14:11 versus 17:9, respectively; $P = .57$).

DCE-MR Imaging and ADC Parameters

Results of DCE-MR imaging and ADC analyses are summarized in the Table. A pulsed input pattern was observed in the arterial input function curves in all patients. nVp, nK^{trans}, nAUC, and nWI were significantly higher in patients with recurrence than in those with benign posttreatment change (nVp: median, 7.00 [range, 0.50–17.33] versus 2.02 [range, 0.33–14.33]; $P = .003$; nK^{trans}: median, 3.87 [range, 0.66–101.00] versus 1.27 [range, 0.03–8.00]; $P < .001$; nAUC: median, 3.34 [range, 1.31–20.81] versus 1.39 [range, 0.01–9.96]; $P < .001$; nWI: median, 4.13 [range, 0.99–20.17] versus 1.70 [range, 0.07–32.48], respectively; $P < .001$). The cutoff value of nVp was 3.68 (sensitivity, 0.69; specificity, 0.76; AUROCC, 0.74 [95% CI, 0.76–0.92]); that of nK^{trans} was 3.02 (sensitivity, 0.85; specificity, 0.64; AUROCC, 0.79 [95% CI, 0.67–0.91]); that of nAUC was 2.04 (sensitivity, 0.69; specificity, 0.88; AUROCC, 0.80 [95% CI, 0.68–0.92]); and that of nWI was 2.69 (sensitivity, 0.69; specificity, 0.84; AUROCC, 0.79 [95% CI, 0.66–0.92]) (Fig 3A, -B). No significant difference was found in nVe, nKep, and nWO between the recurrence and benign

posttreatment change groups. $nADC_{mean}$ was significantly lower in patients with recurrence than in those with benign posttreatment change (recurrence: median, 1.31 [range, 0.77–1.65] versus benign posttreatment change, 2.07 [range, 1.39–3.04]; $P < .001$). The cutoff value of $nADC_{mean}$ was 1.65 (sensitivity, 0.92; specificity, 1.00; AUROCC, 0.97 [95% CI, 0.93–1]). Representative MR images of recurrence and benign posttreatment changes are demonstrated in Figs 1 and 2 and the Online Supplemental Data.

FIG 1. A case of head and neck cancer recurrence. A 72-year-old man after an operation and radiation therapy for squamous cell carcinoma of the floor of the mouth. The left side of the floor of the mouth shows some high signal intensity (*arrows*) on T2WI (*A*) and mild enhancement (*dotted arrows*) on postcontrast fat-suppressed T1WI (*B*). The ADC map (*C*) shows low signal (*arrowheads*), with an $nADC_{mean}$ of 1.38. DCE-MR imaging (*D*, Vp; *E*, Ve; *F*, K^{trans}) shows increased parameters (*thick arrows*), with an nVp of 7.33, nVe of 3.93, and nK^{trans} of 5.44.

FIG 2. Benign posttreatment change of head and neck cancer in a 64-year-old woman after surgery and radiation therapy for mucoepidermoid carcinoma of the left parotid gland. The left parotid surgical bed shows low signal intensity (*arrow*) on T2WI (*A*) and mild enhancement (*dotted arrow*) on postcontrast fat-suppressed T1WI (*B*). The ADC map (*C*) shows no prominent low signal (*arrowhead*), with an $nADC_{mean}$ of 1.75. DCE-MR imaging (*D*, Vp; *E*, Ve; *F*, K^{trans}) shows no increased parameters (*thick arrows*) with an nVp of 0.33, nVe of 0.33, and nK^{trans} of 0.03.

Diagnostic Performance

The AUROCC of the combination of normalized quantitative and semiquantitative DCE-MR imaging parameters with significance (nVp, nK^{trans}, nAUC, and nWI) was 0.81 (95% CI, 0.69–0.93) (Fig 3C). Furthermore, the AUROCC of the combination of normalized DCE-MR imaging parameters with significance (nVp, nVe, nK^{trans}, nAUC, and nWI) and $nADC_{mean}$ was 0.97 (95% CI, 0.93–1) (Fig 3C).

DISCUSSION

This study evaluated the characteristics and differences of normalized parameters of dynamic contrast-enhanced perfusion MR imaging and DWI-ADC between recurrence and posttreatment changes in head and neck cancer. Normalized quantitative DCE-MR imaging parameters (nVp and nK^{trans}), normalized semiquantitative DCE-MR imaging parameters (nAUC and nWI), and $nADC_{mean}$ were significantly different between the recurrence and benign posttreatment change groups. The combined AUROCC was as high as 0.97 when using these parameters to differentiate recurrence and benign posttreatment changes.

DCE-MR imaging is a type of perfusion imaging technique that uses contrast media, and studies using quantitative parameters in head and neck cancer play important roles in the prediction of tumor hypoxia[6,7] and treatment response,[8,9] determination of treatment response,[10,11] and differentiation between recurrence and posttreatment changes.[12] The utility of semiquantitative parameters on DCE-MR imaging in differentiating head and neck cancer recurrence from posttreatment changes[13,14] and that of quantitative parameters, such as permeability surface area and blood volume,[12] are in agreement with the results of this study. Although these studies and the present study have both used semiquantitative and quantitative parameters, the reliability of semiquantitative parameters cannot be guaranteed, especially when the protocols are different.[23] To compensate for this disadvantage, statistical processing using normalized DCE-MR imaging parameters was performed in this study, and significant differences were confirmed for many of the normalized DCE-MR imaging parameters. If we used normalized data, our results are expected to be reproducible in many other institutions that use DCE-MR imaging if the imaging is
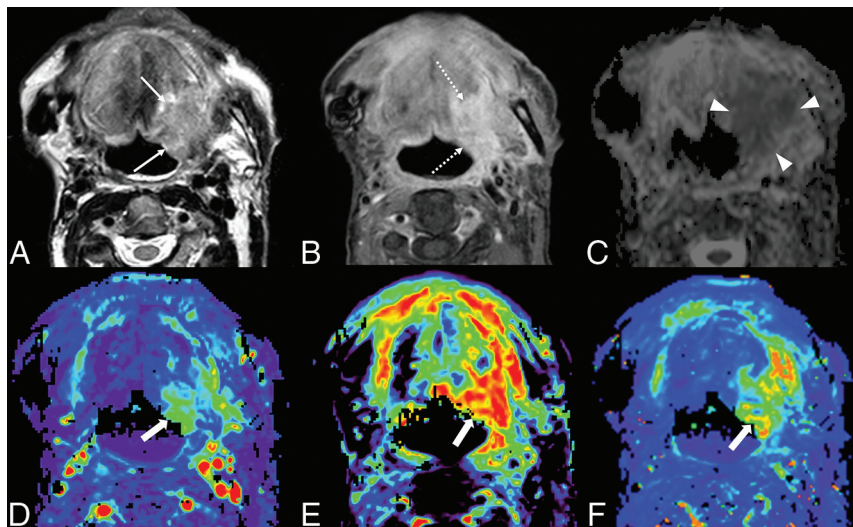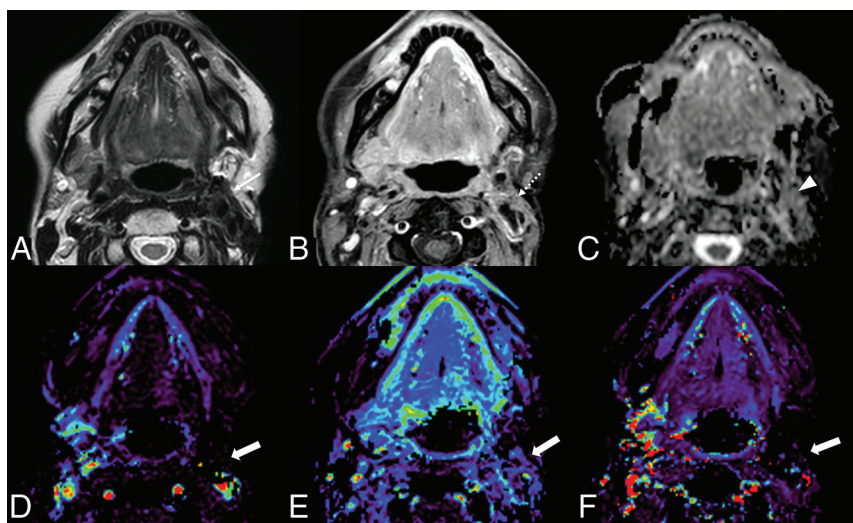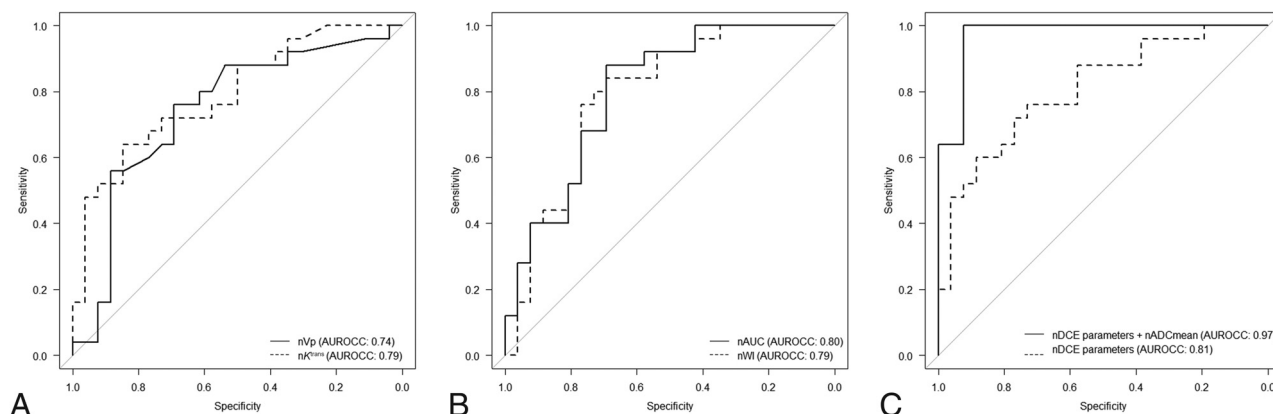
FIG 3. Receiver operating characteristic curves. AUROCCs for nVp (*solid line*) and nK^{trans} (*dashed line*) are 0.74 and 0.79, respectively (*A*). AUROCCs for nAUC (*solid line*) and nWI (*dashed line*) are 0.80 and 0.79, respectively (*B*). AUROCCs for the combination of normalized DCE-MR imaging parameters (nVp, nK^{trans}, nAUC, and nWI) (*dashed line*) and the combination of normalized DCE-MR imaging parameters and nADC$_{mean}$ (*solid line*) are 0.81 and 0.97, respectively (*C*).

performed with the same protocol. In addition, this study used relatively new vascular permeability parameters, such as Vp, Ve, K^{trans}, and Kep, and their usefulness in differentiating recurrence from benign posttreatment changes has not been previously reported.

Previous studies have shown that ADC values in recurrent head and neck cancer lesions are lower than those after benign posttreatment changes,[18-20] consistent with the results in the present study. The use of normalized ADCs in the present study and the aforementioned normalized DCE-MR imaging parameters is expected to be reproducible in other institutions by minimizing the effects of several factors that may affect the ADC values such as differences in MR imaging scanners, magnetic field strength, and patient variability.[24]

In the present study, the AUROCC of the combined normalized DCE-MR imaging parameters was high (0.81). The normalized DCE-MR imaging parameters (nVp, nK^{trans}, nAUC, and nWI), which showed significant differences in the present study, should be evaluated comprehensively rather than separately to be more effective in differentiating head and neck cancer recurrence from benign posttreatment changes. Furthermore, the combined normalized DCE-MR imaging parameters and nADC$_{mean}$ that showed a significant difference in the present study showed a high AUROCC value of 0.97. Notably, [^{18}F] FDG-PET/CT has very high specificity and sensitivity for differentiating head and neck cancer recurrences from posttreatment changes,[25] with a high AUROCC of 0.975,[26] which is comparable with an AUROCC of 0.97 for the combined evaluation of normalized DCE parameters and nADC$_{mean}$ in the present study. Although this study demonstrated the usefulness of normalized DCE parameters and nADC$_{mean}$, further study is needed to determine whether they can be used as a substitute for PET/CT. PET/CT has advantages over MR imaging such as the ability to detect systemic metastases. On the contrary, MR imaging has advantages such as superior spatial and tissue resolution and better medical cost.

There are several limitations in the present study. First, this was a single-center retrospective study. Second, the pathology of the included cases was heterogeneous, with only 51% of squamous cell carcinoma (typical of head and neck cancer) and salivary gland tumor cases included. Future studies with homogeneous cases of pathology are warranted. Third, MR imaging scanners were used with different field strengths for image acquisition. However, using normalized DCE-MR imaging and ADC parameters, we might minimize the risk of parameter heterogeneity. In addition, the analyses of the diagnostic performance in this study were optimistic because out-of-sample testing was not performed.

CONCLUSIONS

Normalized quantitative and semiquantitative DCE-MR imaging parameters and ADC values effectively assessed the difference between recurrence and benign posttreatment changes in head and neck cancer. The diagnostic performance of the combination of normalized DCE-MR imaging parameters and ADC values was very high and expected to be reproducible and effective in clinical practice.

Disclosure forms provided by the authors are available with the full text and PDF of this article at www.ajnr.org.

REFERENCES

1. Wong LY, Wei WI, Lam LK, et al. **Salvage of recurrent head and neck squamous cell carcinoma after primary curative surgery.** *Head Neck* 2003;25:953–59 CrossRef Medline
2. Hermans R. **Posttreatment imaging in head and neck cancer.** *Eur J Radiol* 2008;66:501–11 CrossRef Medline
3. Saito N, Nadgir RN, Nakahira M, et al. **Posttreatment CT and MR imaging in head and neck cancer: what the radiologist needs to know.** *Radiographics* 2012;32:1261–82 CrossRef Medline
4. Baba A, Ojiri H, Ikeda K, et al. **Essentials on oncological imaging: postoperative computed tomography and magnetic resonance imaging of oral tongue cancer.** *Can Assoc Radiol J* 2018;69:458–67 CrossRef Medline
5. Aiken AH, Rath TJ, Anzai Y, et al. **ACR Neck Imaging Reporting and Data Systems (NI-RADS): a White Paper of the ACR NI-RADS Committee.** *J Am Coll Radiology* 2018;15:1097–108 CrossRef Medline
6. Newbold K, Castellano I, Charles-Edwards E, et al. **An exploratory study into the role of dynamic contrast-enhanced magnetic resonance imaging or perfusion computed tomography for detection of intratumoral hypoxia in head-and-neck cancer.** *Int J Radiat Oncol Biol Phys* 2009;74:29–37 CrossRef Medline

7. Jansen JF, Carlson DL, Lu Y, et al. **Correlation of a priori DCE-MRI and 1H-MRS data with molecular markers in neck nodal metastases: initial analysis.** *Oral Oncol* 2012;48:717–22 CrossRef Medline

8. Bernstein JM, Kershaw LE, Withey SB, et al. **Tumor plasma flow determined by dynamic contrast-enhanced MRI predicts response to induction chemotherapy in head and neck cancer.** *Oral Oncol* 2015;51:508–13 CrossRef Medline

9. Ng S, Lin C, Chan S, et al. **Dynamic contrast-enhanced MR imaging predicts local control in oropharyngeal or hypopharyngeal squamous cell carcinoma treated with chemoradiotherapy.** *PLoS One* 2013;8: e72230 CrossRef Medline

10. Chikui T, Kitamoto E, Kawano S, et al. **Pharmacokinetic analysis based on dynamic contrast-enhanced MRI for evaluating tumor response to preoperative therapy for oral cancer.** *J Magn Reson Imaging* 2012;36:589–97 CrossRef Medline

11. Tomura N, Omachi K, Sakuma I, et al. **Dynamic contrast-enhanced magnetic resonance imaging in radiotherapeutic efficacy in the head and neck tumors.** *Am J Otolaryngol* 2005;26:163–67 CrossRef Medline

12. Ishiyama M, Richards T, Parvathaneni U, et al. **Dynamic contrast-enhanced magnetic resonance imaging in head and neck cancer: differentiation of new H&N cancer, recurrent disease, and benign posttreatment changes.** *Clin Imaging* 2015;39:566–70 CrossRef Medline

13. Furukawa M, Parvathaneni U, Maravilla K, et al. **Dynamic contrast-enhanced MR perfusion imaging of head and neck tumors at 3 Tesla.** *Head Neck* 2013;35:923–29 CrossRef Medline

14. Semiz Oysu A, Ayanoglu E, Kodalli N, et al. **Dynamic contrast-enhanced MRI in the differentiation of posttreatment fibrosis from recurrent carcinoma of the head and neck.** *Clin Imaging* 2005;29:307–12 CrossRef Medline

15. Ota Y, Liao E, Kurokawa R, et al. **Diffusion-weighted and dynamic contrast-enhanced MRI to assess radiation therapy response for head and neck paragangliomas.** *J Neuroimaging* 2021;31:1035–43 CrossRef Medline

16. Ailianou A, Mundada P, De Perrot T, et al. **MRI with DWI for the detection of posttreatment head and neck squamous cell carcinoma: why morphologic MRI criteria matter.** *AJNR Am J Neuroradiol* 2018;39:748–55 CrossRef Medline

17. Jajodia A, Aggarwal D, Chaturvedi AK, et al. **Value of diffusion MR imaging in differentiation of recurrent head and neck malignancies from post treatment changes.** *Oral Oncol* 2019;96:89–96 CrossRef Medline

18. Tshering Vogel DW, Zbaeren P, Geretschlaeger A, et al. **Diffusion-weighted MR imaging including bi-exponential fitting for the detection of recurrent or residual tumour after (chemo)radiotherapy for laryngeal and hypopharyngeal cancers.** *Eur Radiol* 2013;23:562–69 CrossRef Medline

19. Hwang I, Choi SH, Kim YJ, et al. **Differentiation of recurrent tumor and posttreatment changes in head and neck squamous cell carcinoma: application of high b-value diffusion-weighted imaging.** *AJNR Am J Neuroradiol* 2013;34:2343–48 CrossRef Medline

20. Baba A, Kurokawa R, Kurokawa M, et al. **ADC for differentiation between benign post-treatment changes and recurrence in head and neck cancer: a systematic review and meta-analysis.** *AJNR Am J Neuroradiol* 2022;43:442–47 CrossRef

21. Koontz NA, Wiggins RH. **Differentiation of benign and malignant head and neck lesions with diffusion tensor imaging and DWI.** *AJR Am J Roentgenol* 2017;208:1110–15 CrossRef Medline

22. Mouridsen K, Christensen S, Gyldensted L, et al. **Automatic selection of arterial input function using cluster analysis.** *Magn Reson Med* 2006;55:524–31 CrossRef Medline

23. Donato H, França M, Candelária I, et al. **Liver MRI: from basic protocol to advanced techniques.** *Eur J Radiol* 2017;93:30–39 CrossRef Medline

24. Ding X, Xu H, Zhou J, et al. **Reproducibility of normalized apparent diffusion coefficient measurements on 3.0-T diffusion-weighted imaging of normal pancreas in a healthy population.** *Medicine (Baltimore)* 2019;98:e15104 CrossRef Medline

25. Isles MG, McConkey C, Mehanna HM. **A systematic review and meta-analysis of the role of positron emission tomography in the follow up of head and neck squamous cell carcinoma following radiotherapy or chemoradiotherapy.** *Clin Otolaryngol* 2008;33:210–22 CrossRef Medline

26. Kim S, Roh J, Seung J, et al. **18F-FDG PET/CT surveillance for the detection of recurrence in patients with head and neck cancer.** *Eur J Cancer* 2017;72:62–70 CrossRef Medline